

# STATUS OF ATMOSPHERIC CORRECTION USING A MODTRAN4-BASED ALGORITHM

Michael W. Matthew,<sup>1</sup> Steven M. Adler-Golden,<sup>1</sup> Alexander Berk,<sup>1</sup> Steven C. Richtsmeier,<sup>1</sup> Robert Y. Levine,<sup>1</sup>  
Lawrence S. Bernstein,<sup>1</sup> Prabhat K. Acharya,<sup>1</sup> Gail P. Anderson,<sup>2</sup> Gerry W. Felde,<sup>2</sup> Michael P. Hoke,<sup>2</sup>  
Anthony Ratkowski,<sup>2</sup> Hsiao-Hua Burke,<sup>3</sup> Robert D. Kaiser,<sup>4</sup> and David P. Miller<sup>4</sup>

## 1. INTRODUCTION

Atmospheric correction (or compensation) of AVIRIS or other spectral imagery refers to the retrieval of surface reflectance spectra from measured radiances. Several methods for doing this are described in the literature. The simplest and by far the computationally fastest is the "Empirical Line Method" (ELM). It assumes that the radiance image contains some pixels with a known reflectance spectrum, and also that the radiance and reflectance values for each wavelength channel of the sensor are linearly related; therefore, the image can be converted to reflectance by applying a simple gain and offset derived from the known pixels. The ELM is however not generally applicable, as known reflectances are often not available, and the linearity assumption, which presumes uniform atmospheric transmission, scattering and adjacency effects throughout the scene, may not be accurate. Therefore, alternative atmospheric correction methods based on first-principles radiation transport modeling have been developed. Algorithms applicable to AVIRIS scenes over land include ATREM (Gao et al, 1996), the method of (Green *et al.* 1996), which requires additional input from a calibration image, and an algorithm recently developed by Spectral Sciences, Inc. (SSI) and the Air Force Research Laboratory (AFRL) (Adler-Golden *et al.*, 1999) that is based on the MODTRAN4 radiation transport model (Berk *et al.*, 1998). This paper summarizes the current status of the SSI/AFRL algorithm and briefly describes recent upgrades, which include automated aerosol retrieval, cloud masking, speed improvements, and a MODTRAN4 upgrade to correct recently discovered water line parameter errors (Giver *et al.*, 2000).

## 2. METHODOLOGY

### 2.1 Review of Basic Method

A brief review of the AFRL/SSI atmospheric correction method is presented. We start from a standard equation for spectral radiance at a sensor pixel,  $L^*$ , that applies to the solar wavelength range (thermal emission is neglected) and flat, Lambertian materials or their equivalents. The equation can be written as (Vermote *et al.*, 1994)

$$L^* = Ap/(1-\rho_e S) + B\rho_e/(1-\rho_e S) + L^*_a \quad (1)$$

Here  $\rho$  is the pixel surface reflectance,  $\rho_e$  is an average surface reflectance for the pixel and a surrounding region,  $S$  is the spherical albedo of the atmosphere,  $L^*_a$  is the radiance backscattered by the atmosphere, and  $A$  and  $B$  are coefficients that depend on atmospheric and geometric conditions but not on the surface. Each of these variables depends on the spectral channel; the wavelength index has been omitted for simplicity. The first term in Equation (1) corresponds to radiance that is reflected from the surface and travels directly into the sensor, while the second term corresponds to radiance from the surface that is scattered by the atmosphere into the sensor. The distinction between  $\rho$  and  $\rho_e$  accounts for the "adjacency effect" (spatial mixing of radiance among nearby pixels) caused by atmospheric scattering. The adjacency effect correction may be ignored by setting  $\rho_e = \rho$ . However, this can result in significant reflectance errors at short wavelengths, especially under hazy conditions and when there are strong contrasts among the materials in the scene (Adler-Golden *et al.*, 1999).

---

<sup>1</sup> Spectral Sciences, Inc., 99 South Bedford St., Burlington, MA 01803 (matthew@spectral.com)

<sup>2</sup> Air Force Research Laboratory, Space Vehicles Directorate, Hanscom AFB, MA 01731

<sup>3</sup> MIT Lincoln Laboratory, Lexington, MA 02173

<sup>4</sup> Spectral Information Technical Application Center (SITAC), Fairfax, VA 22033

The values of  $A$ ,  $B$ ,  $S$  and  $L_a^*$  are determined from MODTRAN4 calculations that use the viewing and solar angles and the mean surface elevation of the measurement and assume a certain model atmosphere, aerosol type, and visible range. The values of  $A$ ,  $B$ ,  $S$  and  $L_a^*$  are strongly dependent on the water vapor column amount, which is generally not well known and may vary across the scene. To account for unknown and variable column water vapor, the MODTRAN4 calculations are looped over a series of different column amounts, then selected wavelength channels of the image are analyzed to retrieve an estimated amount for each pixel. Specifically, radiance averages are gathered for two sets of channels, an "absorption" set centered at a water band (typically the 1.13  $\mu\text{m}$  band) and a "reference" set of channels taken from just outside the band. A 2-dimensional look-up table (LUT) for retrieving the water vapor from these radiances is constructed. One dimension of the table is the reference to absorption ratio and the other is the reference radiance. The second dimension accounts for a reflectance-dependent variation in the ratio arising from the different amounts of absorption in the atmospherically-scattered and surface-reflected components of the radiance. After the water retrieval is performed, Equation (1) is solved for the pixel surface reflectances in all of the sensor channels. The solution method (Richter, 1996; Vermote *et al.*, 1997) involves computing a spatially averaged radiance image  $L_e^*$ , from which the spatially averaged reflectance  $\rho_e$  is estimated using the approximate equation

$$L_e^* \approx (A+B)\rho_e/(1-\rho_e S) + L_a^* \quad (2)$$

The spatial averaging is performed using a point-spread function that describes the relative contributions to the pixel radiance from points on the ground at different distances from the direct line of sight. The SSI/AFRL algorithm approximates this function as a radial exponential.

In the above discussion it has been assumed that the quantity of aerosol or haze in the scene has been adequately estimated. As described previously (Adler-Golden *et al.*, 1999), the SSI/AFRL algorithm includes a method for retrieving an estimated aerosol/haze amount from one or more reference surfaces in the scene that have a known reflectance in some wavelength bandpass. Best results are obtained using short (visible) wavelengths and either a very dark surface, such as vegetation or deep calm water, or a very bright surface, such as a white calibration target that is large enough to fill a whole pixel. In this method, calculations to determine  $A$ ,  $B$ ,  $S$  and  $L_a^*$  are carried out for the spectral channels in the designated bandpass. Instead of iterating over different water vapor values, these calculations are performed over a series of visible ranges, e.g. 200, 100, 50, 33, 25, 20 and 17 km, that are evenly spaced in their reciprocals (optical depths). The user selects the reference pixels and assigns them a mean reflectance value for the selected channels. The algorithm derives a visible range for each reference pixel by interpolating from a 2-D LUT that depends on  $L$  and  $L_e^*$ . From these results an average or other "best" estimate of the visible range can be derived and used for the MODTRAN4 calculation loop over water vapor.

An example of AVIRIS data processed with the above procedure is shown in Figure 1. The data are of white and black calibration panels at the Stennis Space Center, and were acquired from the low altitude (Twin Otter) platform in October, 1998. After adjusting the wavelength calibration slightly and performing the atmospheric correction, the spectra were smoothed using a "polishing" algorithm (Adler-Golden *et al.*, 1999; Boardman, 1998). The AVIRIS spectra (particularly the white panel) show some absorption residuals adjacent to the cut-out regions of very strong water absorption and also at the 0.94  $\mu\text{m}$  water band, but on the whole the agreement with the "ground truth" spectra is good. The  $\sim 0.01$  difference between the black panel spectra is within the variability and uncertainty in the ground truth measurement.

## 2.2 Limitations

The basic atmospheric correction method described above, as well as those in other first-principles codes such as ATREM, work well in many but not all scenes. In particular, they require cloud-free conditions, the presence of at least one material in the scene with a known reflectance at a visible wavelength, and sufficient computing time to perform tens of mathematical operations per image pixel per wavelength channel.

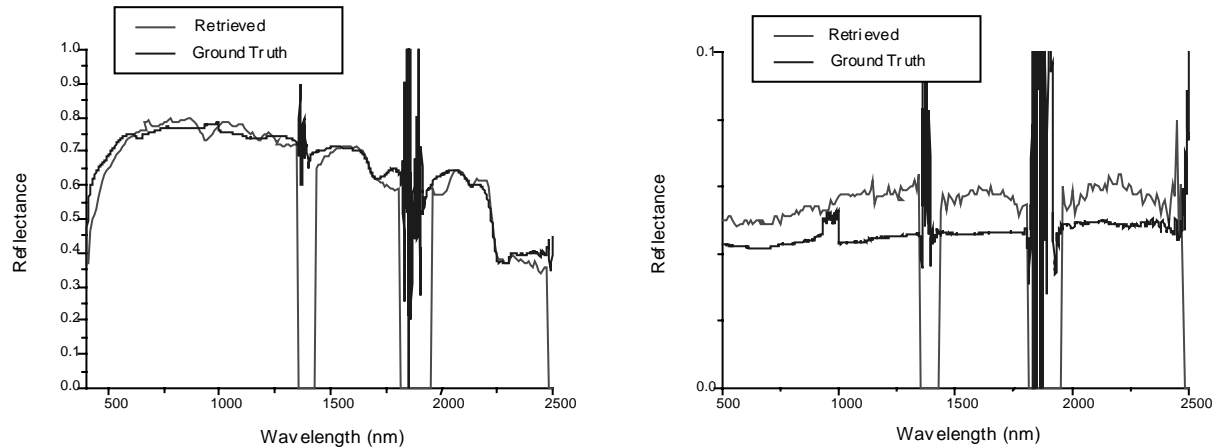


Figure 1. Comparisons of Atmospherically Corrected AVIRIS Data with Ground Truth Measurements for White (left) and Black (right) Calibration Panels at the Stennis Space Center.

*Cloud Effects.* Clouds and cloud shadows pose several problems for atmospheric correction. Not only do cloud-contaminated pixels have incorrect reflectance, they also can degrade the reflectance accuracy in other parts of the scene. This is because clouds impact the spatially averaged radiance  $L^*_e$  used in Equation (2) to generate  $\rho_e$  for the adjacency correction. According to theory,  $\rho_e$  should account only for reflecting material that is below the scattering atmosphere. While clouds typically lie below most of the molecular (Rayleigh) scattering, which is important at the very shortest (blue-violet) wavelengths, they typically lie above the aerosol and haze layers that dominate the scattering in the rest of the spectrum. Since clouds are typically much brighter than the terrain,  $\rho_e$  is overestimated, leading to underestimated surface reflectance retrievals. Therefore it is important to identify and remove cloud-contaminated pixels prior to the calculation of  $\rho_e$ . Cloud shadows also produce reflectance errors; however, their effects on material identification can be compensated to some extent, and their impact on clear parts of the scene is minimal.

*Absence of Accurately Known Surfaces.* For the purpose of aerosol/haze amount retrieval, vegetation, water, or other dark surfaces can frequently be identified in a scene. However, reflectance values for these surfaces at appropriate wavelengths are often not known to within the accuracy needed (around 0.01 reflectance units or better) for a good retrieval. Even with "calibrated" surfaces the reflectance may not be known to within this accuracy because of complications caused by non-Lambertian bidirectional reflectance distribution functions. However, a method based on a known reflectance ratio for different wavelengths, such as the (Kaufman *et al.* 1997) dark pixel method, can minimize these problems.

*Computing Time Requirements.* For a typical image containing several hundred or more spectral channels and hundreds of thousands of pixels or more, the speed of the atmospheric correction is fundamentally limited by the mathematical operations required to generate the reflectance values for each pixel and channel from the Equation (1) parameters. Current algorithms, such as ATREM and the SSI/AFRL code, that use pixel-specific values of water vapor (and possibly other quantities such as  $\rho_e$ ) require tens of operations per pixel-channel. Most of the operations are consumed in interpolating to find the appropriate  $A$ ,  $B$ ,  $S$  and  $L^*_a$  parameters for each pixel. A more efficient procedure is needed to achieve high-speed atmospheric correction.

*Model Accuracy.* Any first-principles atmospheric correction method is necessarily limited by the accuracy of its radiation transport model. We have recently had opportunities to validate MODTRAN4 against analytical and Monte Carlo scattering calculations as well as against "exact" line-by-line transmittance calculations degraded to AVIRIS spectral resolution. Excellent agreement was obtained in each case. However, consistency among calculations does not guarantee an accurate representation of reality. Recently, it has been discovered that a number of bands of water vapor in the HITRAN atlas (Rothman *et al.*, 1998), upon which MODTRAN4 as well as line-by-line codes are based, have incorrect line strengths. In the 0.94  $\mu\text{m}$  band the errors are around 14%, and significantly impact the atmospheric correction. These errors have been corrected in the most recent version of MODTRAN4.

Other known deficiencies in MODTRAN4 include the omission of certain collision-induced absorption bands of oxygen (Solomon *et al.*, 1998).

### 3. UPGRADES

The AFRL/SSI atmospheric correction code has been upgraded with several new algorithms that address, if not completely solve, the abovementioned limitations:

- A new method has been implemented for retrieving the aerosol/haze amount from an assumed ratio of in-band reflectances, rather than from an assumed reflectance value. This method can utilize user-selected pixels or can automatically find suitable dark terrain pixels (Kaufman *et al.*, 1997) for the retrieval.
- An algorithm for identifying cloud-containing pixels in AVIRIS or similar data has been implemented, and is used to improve the calculation of  $L_e^*$  and  $\rho_e$  in Equations (1) and (2). Since this algorithm requires a prior water vapor retrieval, the order and number of steps in the atmospheric correction process has been altered.
- A new method has been developed that greatly reduces the number of mathematical operations required to generate the reflectance values once the atmospheric parameters have been defined. The method operates by averaging the water vapor and  $\rho_e$  values over small groups of neighboring pixels, so that the same  $A$ ,  $B$ ,  $S$ , and  $L_a^*$  parameters may be assigned to all pixels in the group.

These upgrades are described in more detail below. In addition, we show an example of the impact of the water line strength revisions on a reflectance retrieval.

#### 3.1 Aerosol Retrieval Method

A general reflectance ratio-based algorithm has been developed for retrieving an aerosol amount (i.e., the visible range). The reference pixels can be chosen by the user, or dark pixels can be selected automatically based on a specified maximum reflectance. To implement the (Kaufman *et al.* 1997) method, one chooses bandpasses centered at 0.66  $\mu\text{m}$  and 2.1  $\mu\text{m}$ , a reflectance ratio of  $\sim 0.5$ , and a 2.1  $\mu\text{m}$  reflectance maximum of around 0.1.

Radiance images in each of the two bandpasses are assembled from both the original data cube and from the spatially averaged radiance  $L_e^*$ . MODTRAN4 calculations are conducted to determine  $A$ ,  $B$ ,  $S$  and  $L_a^*$  for a series of trial visible range values. For each visible range and reference pixel, the reflectance solutions for the two bandpasses are calculated, and the reflectance error for the shorter-wavelength bandpass (the difference between the calculated reflectance and the calculated longer-wavelength reflectance times the assumed ratio) is tabulated. A visible range estimate for each selected pixel can be obtained by interpolating within the resulting array of reflectance errors to find the value that yields zero error. To more efficiently calculate a scene-average visible range, the reflectance error arrays are averaged over all reference pixels, and the interpolation is performed on the result.

We have tested this method using different reference materials and data from two different imaging sensors, including AVIRIS. Using calibration panels as reference pixels, the visible range results were compared with results from the original reflectance-based method, and very good agreement was found. Using natural dark terrain, results were assessed for different reflectance cutoffs and ratio values within the tolerances found by (Kaufman *et al.* 1997). Our preliminary analysis indicates that the typical obtainable retrieval accuracy is 0.01 to 0.02 per km for 1/(visible range). For example, the difference between retrieved visible ranges values of 50 km and 300 km may not be significant, whereas the differences between values of 20 km and 50 km or 13 km and 20 km would be considered significant. In some cases the results can be made less sensitive to the value of the reflectance ratio by choosing a very low reflectance cutoff, such as 0.04, for the dark pixel selection. However, for scenes containing shallow or turbid water bodies a low cutoff can produce anomalous results, since the low cutoff favors the selection of the water pixels, which can have a very different reflectance ratio than dark land pixels. A more sophisticated pixel selection

method, such as one that includes both maximum and minimum reflectance cutoffs to discriminate against surface water, should provide better results.

### 3.2 Identification and Utilization of Cloud-Containing Pixels

An algorithm has been developed for generating a cloud "mask" that identifies cloud-containing pixels in the scene. At the present time the main uses of the cloud mask in the SSI/AFRL atmospheric correction code are (1) to indicate regions where the atmospheric correction is invalid or suspect, and (2) to flag pixels that need to be removed from the calculation of  $L^*_e$  (currently these pixels are replaced by the scene average radiance). While it is most important to flag bright, opaque clouds, it is also desirable to find pixels that contain appreciable cirrus or other thin cloud cover.

A number of cloud detection algorithms have been developed based on multispectral data. A comprehensive review is presented by Ackerman *et al.* (1998), who developed an algorithm for the MODIS sensor. Their algorithm uses a combination of tests, including (1) a color balance test based on a SWIR/red reflectance ratio ( $0.9 < \rho(0.87 \mu\text{m}) / \rho(0.66 \mu\text{m}) < 1.1$  indicates clouds), (2) a reflectance test at  $0.94 \mu\text{m}$  (a high signal correlates with low column water vapor, hence reflection from a bright, elevated object), and (3) a variety of brightness tests at IR wavelengths. In a paper on simple algorithms for multispectral atmospheric correction, (Borel *et al.* 1999) discuss an analogue to the SWIR/red ratio test that combines an upper threshold on the NDVI (Normalized Differential Vegetation Index) with a lower threshold on the SWIR bandpass (i.e., a brightness test). They also describe a water vapor absorption test involving a continuum interpolated band ratio (CIBR).

With AVIRIS there is no IR coverage past  $2.5 \mu\text{m}$ , but there is high spectral resolution that permits a very good column water vapor retrieval. Therefore, following Ackerman and Borel, we devised a cloud mask based on combining tests for brightness, color balance, and low column water in the visible and SWIR regions. Because of processing time constraints, it is advantageous to utilize bands that are already being gathered by the atmospheric correction code for other purposes (e.g.,  $2.1 \mu\text{m}$ ,  $1.13 \mu\text{m}$  water absorption and reference bandpasses,  $0.66 \mu\text{m}$ , red, blue, and green bandpasses used for image display) and to use the retrieved water vapor amounts. From these data we implemented analogues of the tests described above.

From the standpoint of clear-sky atmospheric correction, the main effect of clouds in the scene arises from the adjacency effect compensation, which requires a spatially smoothed radiance. It is not appropriate to include cloudy pixels in the smoothed radiance, which means that the cloud mask must be determined prior to both the aerosol retrieval and the atmospheric correction. A cloud test based on water vapor must use some assumed aerosol amount, and a test based on reflectances cannot include the adjacency effect compensation. Given these requirements, the preferred sequence of steps for the atmospheric correction process is as follows:

1. Initial water vapor retrieval. A nominal visible range (e.g., 50 km) is assumed.
2. Cloud mask generation. Brightness and color balance tests are applied to establish probable clear pixels, and a spatially average water vapor average is taken. Pixels containing significantly lower water vapor than this spatial average are identified, and the results of this test and the other tests are combined to define the opaque cloud mask.
3. Spatial averaging of the radiance using the adjacency effect point-spread function. Prior to averaging, the scene-average radiance replaces the actual radiance in the cloud-masked pixels.
4. Aerosol (visible range) retrieval. The automated ratio-based algorithm is used with adjacency correction (both the smoothed and unsmoothed radiances are input).

5. Refined water vapor retrieval. The derived visible range and perhaps a narrowed range of water column amounts are used.
6. The cloud mask may be recalculated, but it should not be much different than before.
7. Full reflectance spectrum retrieval.

A convenient method for the cloud mask generation, incorporated in the most recent version of the SSI/AFRL atmospheric correction method, is outlined below. Brightness, color balance, and water vapor tests are used together to define a mask for "ordinary", low-altitude clouds. In addition, 1.38  $\mu\text{m}$  data are used to define a separate mask for high-altitude (i.e., cirrus) clouds, following the work of Gao and co-workers (1998, 1993).

The brightness test requires that an atmospheric correction from radiance to reflectance units be performed for at least one sensor bandpass. Since the water reference reflectance channel average (taken from either side of 1.13  $\mu\text{m}$ ) and a corresponding reflectance are already generated, it can be used for the brightness test. Borel *et al.* (1999) recommend a reflectance lower threshold of around 0.3 for clouds in the SWIR. We have obtained good results with a similar value, 0.4.

The color balance test involves comparing at least two bandpasses at different wavelengths. One bandpass can be the water reference, the second can be a visible bandpass, preferably green wavelengths, properly scaled. The test outcome is positive if the ratio of effective reflectances (radiance divided by the solar function) in the green and water reference bandpasses is unity to within some bounding values. Suitable bounding values determined by trial and error are 0.4 and 1.2.

The low-water test involves comparing the pixel's column water vapor with a threshold value that is derived from pixels that fail both the brightness and color balance tests and therefore are classified as clear. The threshold is defined with respect to a clear-pixel spatial average, obtained by convolving the clear pixel image with a window that is smaller than the image. Ideally, the window should be larger than typical cloud dimensions but smaller than typical large-scale topographic dimensions. For example, for AVIRIS data taken from a 20 km altitude, a suitable window size is around 40 x 40 pixels. The outcome of the low-water test is defined to be positive for a pixel if its column water vapor is less than 85% of the clear-pixel value.

To generate the high cloud mask, one or two channels of data in the center of the 1.38  $\mu\text{m}$  water band are selected. The data are histogrammed, the maximum of the histogram is assigned to the background level, and pixels whose signals exceed some threshold (presently 0.03  $\mu\text{W}/\text{nm}/\text{cm}^2/\text{sr}$ ) above the background level are flagged. We have found that this method often detects thick, lower-altitude clouds as well as cirrus clouds.

To date, limited testing of the cloud identification algorithm has been conducted. An application to an AVIRIS image taken near North Conway, NH is shown in Figure 2. The pixels are color coded according to which cloud tests came out positive. Except where the clouds are extremely thin, all pixels that appear to the eye to be contaminated with clouds are flagged by the algorithm, and false positives are not evident. A low rate of false positives, particularly for the "ordinary" cloud test, has been verified using a variety of cloud-free scenes.

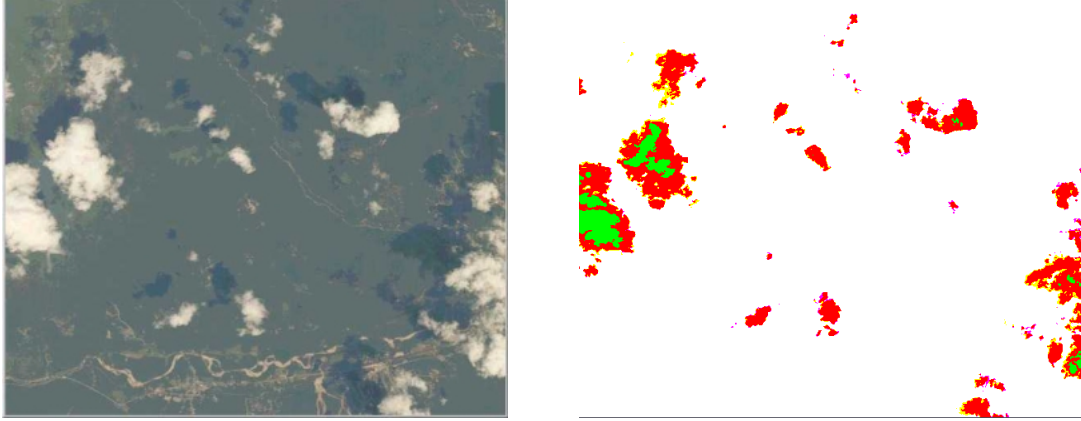


Figure 2. Left, RGB Rendition of AVIRIS Radiance Image. Right, calculated cloud mask. The pixels tested positive as follows: Yellow = high cloud, Violet = "ordinary" cloud, Red = high + "ordinary". Green pixels tested positive for high clouds and also had column water values below the lower limit of the water LUT, indicative of a thick cloud.

### 3.3 Reflectance Calculation Speedup

The reflectance calculation described in Section 2.1 can be made much faster, with little sacrifice in accuracy, by approximating  $A$ ,  $B$ ,  $S$ ,  $L^*_a$  and  $\rho_e$  using average values for a group of nearby pixels (such as an  $N \times N$  array), referred to here as a "superpixel". The method takes advantage of the fact that Equation (1) relating radiance to reflectance can be transformed into the simple linear equation,

$$\rho = mL^* + b \quad (3)$$

where  $m$  and  $b$  are expressed in terms of superpixel values for  $A$ ,  $B$ ,  $S$ ,  $L^*_a$ , and  $\rho_e$ . Suitable values for these parameters are determined by using superpixel-average water vapor amounts to interpolate from MODTRAN4-derived LUTs. The superpixel water vapor amounts may be either averages of the retrievals from individual pixels or retrievals from superpixel-average radiances.  $\rho_e$  is calculated from the value of  $L^*_e$  for the superpixel. Note that since  $L^*_e$  is itself a spatial average, for all practical purposes it does not need to be calculated on a single-pixel basis in the first place. Once  $m$  and  $b$  are defined,  $\rho$  is calculated from  $L^*$  for each pixel.

The speedup in the calculation of the reflectance compared to the standard pixel-by-pixel approach derives from the fact that the interpolations and other mathematical steps required to generate  $m$  and  $b$  (approximately 21 arithmetic operations) are performed only once per  $N \times N$  pixels. In the limit of large  $N$ , the number of operations per pixel-channel reduces to the 2 operations in Equation (3), which are the same as in the Empirical Line Method. Most of the speed benefit can be achieved even with a modest superpixel size, such as  $N = 4$  (see Table 1), which yields only marginal differences with the "exact"  $N = 1$  results.

To date, we have implemented the superpixel method in an IDL language code and obtained a fourfold improvement in speed, to around 1/3 s per line of 614 AVIRIS pixels on a 330 MHz PC. A further order-of-magnitude speedup is anticipated with recoding to a more efficient language such as C or FORTRAN.

**Table 1. Theoretical Number of Floating Point Operations Per Pixel-channel using the Superpixel Method for Calculating Spectral Reflectance.**

Superpixel Dimensions	FLOPs / pixel / channel
1x1	23
2x2	9.25
3x3	4.33
4x4	3.31

### 3.4 Revised Water Line Strengths

A revised HITRAN line list (Rothman *et al.*, 1998), containing the (Giver *et al.* 2000) water line parameter corrections, was used to formulate a new set of water band model parameters for MODTRAN4. The impact of the new parameters on AVIRIS data is shown in Figure 3 for the Stennis Space Center white panel. To best show the residual errors, no spectral "polishing" was applied. The new parameters virtually eliminate the anomalous 0.94  $\mu\text{m}$  absorption which was found earlier, and which has been a persistent artifact in AVIRIS retrievals, especially in moist atmospheres. At most other wavelengths the two sets of results are nearly identical. The new parameters led to a very small increase in the retrieved water column amount, from 1550 to 1570 atm-cm, due to a  $\sim 1\%$  change in the 1.13  $\mu\text{m}$  band strength. Both results are in remarkable (perhaps partly fortuitous) agreement with the value of 1560 atm-cm measured by a radiosonde near the time and location of the AVIRIS flight.

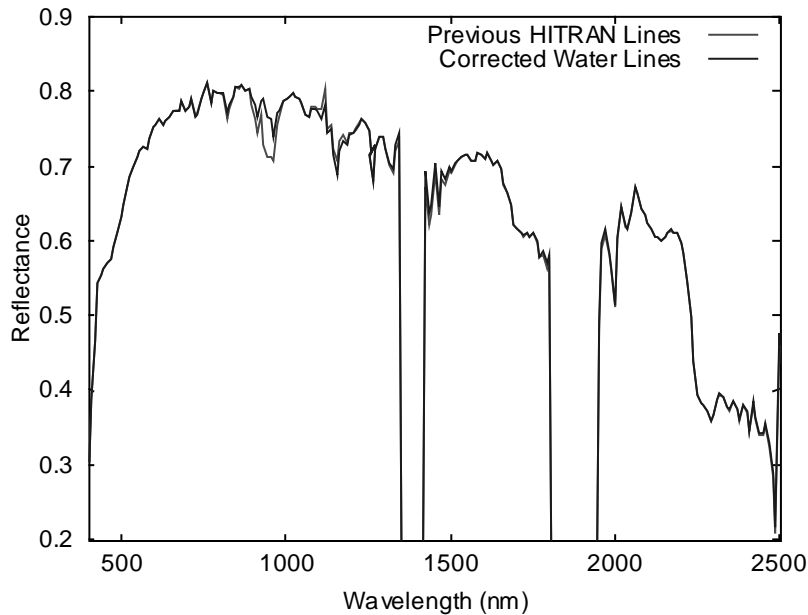


Figure 3. Comparison of White Panel Reflectance Spectra retrieved from AVIRIS Data Using MODTRAN4 with Corrected (blue) and Original (red) HITRAN Water Line Parameters.

## 4. CONCLUSIONS

Considerable progress has been made on several fronts to improve the SSI/AFRL atmospheric correction algorithm's speed, accuracy, and automated application to cloudy and hazy scenes. Work is in progress to develop algorithms that treat cloud or other shadowing effects and that retrieve information on the aerosol type (i.e., particle size distribution and/or single-scattering albedo) as well as amount. The potential also exists to develop an even faster atmospheric correction capability, requiring only a few mathematical operations per pixel-channel, by combining the fast reflectance calculation method described here with a pre-calculated library of MODTRAN4 runs.

This would enable a 512-line AVIRIS data cube to be atmospherically corrected with high accuracy in only a few minutes using a present-day PC.

## 5. ACKNOWLEDGEMENTS

We thank Greg Terrie (NASA SSC) for providing us with AVIRIS data and ground truth measurements and L. Rothman (Harvard-Smithsonian Center for Astrophysics) and S.A. Clough (Atmospheric and Environmental Research, Inc.) for providing the revised HITRAN line list. We gratefully acknowledge support from AFRL and SITAC under USAF Contract No. F19628-98-C-0050, from NASA under SBIR Contract No. NAS13-99014, and from Spectral Sciences, Inc.

## 6. REFERENCES

- Ackerman, S.A., K.I. Strabala, W.P. Menzel, R.A. Frey, C.C. Moeller, and L.E. Gumley, 1998, "Discriminating Clear Sky from Clouds with MODIS," *J. Geophys. Res.* **103**, 32141.
- Adler-Golden, S.M., M.W. Matthew, L.S. Bernstein, R.Y. Levine, A. Berk, S.C. Richtsmeier, P.K. Acharya, G.P. Anderson, G. Felde, J. Gardner, M. Hoke, L.S. Jeong, B. Pukall, A. Ratkowski and H.K. Burke, 1999, "Atmospheric Correction for Short-wave Spectral Imagery Based on MODTRAN4," *Summaries of the Eighth Annual JPL Earth Science Workshop*, Vol. I, available at <http://makalu.jpl.nasa.gov> (similar text available at <http://www.spectral.com>).
- Berk, A., L. S. Bernstein, G. P. Anderson, P. K. Acharya, D. C. Robertson, J. H. Chetwynd and S. M. Adler-Golden, 1998, "MODTRAN Cloud and Multiple Scattering Upgrades with Application to AVIRIS," *Remote Sens. Environ.* **65**, 367.
- Boardman, J.W., "Post-ATREM Polishing of AVIRIS Apparent Reflectance Data using EFFORT: a Lesson in Accuracy versus Precision, 1998, " *Summaries of the Seventh JPL Airborne Earth Science Workshop*, JPL Publication 97-21, Vol. 1, p. 53.
- Borel, C.C., P.V. Villeneuve, W.B. Clodius, J.J. Szymanski, and A.B. Davis, 1999, "Practical Atmospheric Correction Algorithms for a Multi-spectral Sensor from the Visible through the Thermal Spectral Regions," SPIE '99 Paper, Conf. 3717-19, Los Alamos National Laboratory Report No. LA-UR-99-1374.
- Gao, B.-C., Y. J. Kaufman, W. Han, and W. J. Wiscombe, 1998, "Removal of Thin Cirrus Path Radiances in the 0.4 - 1.0  $\mu\text{m}$  Spectral Region Using the 1.375- $\mu\text{m}$  Strong Water Vapor Absorption Channel," *Summaries of the Seventh JPL Airborne Earth Science Workshop*, JPL Publication 97-21, Vol. 1, pp. 121-130.
- Gao, B.-C., A.F.H. Goetz, and W.J. Wiscombe, 1993, "Cirrus Cloud Detection from Airborne Imaging Spectrometer Data Using the 1.38  $\mu\text{m}$  Water Vapor Band," *Geophys. Res. Lett* **20**, 301-304.
- Gao, B.-C., K.B. Heidebrecht and A.F.H. Goetz, 1996, *Atmosphere Removal Program (ATREM) Version 2.0 Users Guide*, Center for the Study of Earth from Space/CIRES, University of Colorado, Boulder, Colorado, 26 pages.
- Giver, L.P., C. Chackerian, Jr., and P. Varanasi, 2000, "Visible and Near-infrared  $\text{H}_2^{16}\text{O}$  Line Intensity Corrections for HITRAN-96," *J. Quant. Spectrosc. Radiat. Transfer*, in press.
- Green, R.O., D.A. Roberts, and J.E. Conel, "Characterization and Compensation of the Atmosphere for Inversion of AVIRIS Calibrated Radiance to Apparent Surface Reflectance, 1996, " *Summaries of the Sixth Annual JPL Airborne Earth Science Workshop*, JPL Publication 96-4, Vol. 1, Pasadena, California, pp. 135-146.
- Kaufman, Y. J., D. Tanre, L. A. Remer, E. F. Vermote, A. Chu, and B. N. Holben, 1997, "Operational Remote Sensing of Tropospheric Aerosol over Land from EOS Moderate Imaging Spectroradiometer," *J. Geophys. Res.* **102**, 17051.
- Kaufman, Y.J., A.E. Wald, L.A. Remer, B.-C. Gao, R.-R. Li, and L. Flynn, 1997, "The MODIS 2.1- $\mu\text{m}$  Channel--Correlation with Visible Reflectance for Use in Remote Sensing of Aerosol," *IEEE Transactions on Geoscience and Remote Sensing*, Vol. 35, pp. 1286-1298.

Richter, R., "Atmospheric Correction of DAIS Hyperspectral Image Data, 1996," *SPIE AEROSENSE '96 Conference*, Orlando, FL, April 8-12, SPIE Proceedings, Vol. 2758.

Rothman, L.S., C.P. Rinsland, A. Goldman, S.T. Massie, D.P. Edwards, J.-M. Flaud, A. Perrin, C. Camy-Peyret, V. Dana, J.-Y. Mandin, J. Schroeder, A. McCann, R.R. Gamache, R.B. Wattson, K. Yoshino, K.V. Chance, K.W. Jucks, L.R. Brown, V. Nemtchinov and P. Varanasi, 1998, "The HITRAN Molecular Spectroscopic Database and HAWKS (HITRAN Atmospheric Workstation): 1996 Edition," *J. Quant. Spectrosc. Radiat. Transfer*, Vol. 60, pp. 665-710.

Solomon, S., R.W. Portmann, R.W. Sanders and J.S. Daniel, 1998, "Absorption of Solar Radiation by Water Vapor, Oxygen and Related Collision Pairs in the Earth's Atmosphere," *J. Geophys. Res.*, Vol. 103, pp. 3847-3858.

Vermote, E.F., D. Tanre, J.L. Deuze, M. Herman and J.J. Morcrette, 1994, *Second Simulation of the Satellite Signal in the Solar Spectrum (6S)*, 6S User Guide Version 6.0, NASA-GSFC, Greenbelt, Maryland, 134 pages.

Vermote, E.F., N. El Saleous, C.O. Justice, Y.J. Kaufman, J.L. Privette, L. Remer, J.C. Roger and D. Tanre, 1997, "Atmospheric Correction of Visible to Middle-Infrared EOS-MODIS Data Over Land Surfaces: Background, Operational Algorithm and Validation," *J. Geophys. Res.*, Vol. 102, pp. 17131-17141.